Hypertension Research (2016) 39, 227–236

www.nature.com/hr

ORIGINAL ARTICLE

# $Ca^{2+}$-regulated lysosome fusion mediates angiotensin II-induced lipid raft clustering in mesenteric endothelial cells

Wei-Qing Han[1,2,3], Wen-Dong Chen[1,3], Ke Zhang[1,2], Jian-Jun Liu[1,3], Yong-Jie Wu[1,3] and Ping-Jin Gao[1,2,3]

**It has been reported that intracellular $Ca^{2+}$ is involved in lysosome fusion and membrane repair in skeletal cells. Given that angiotensin II (Ang II) elicits an increase in intracellular $Ca^{2+}$ and that lysosome fusion is a crucial mediator of lipid raft (LR) clustering, we hypothesized that Ang II induces lysosome fusion and activates LR formation in rat mesenteric endothelial cells (MECs). We found that Ang II acutely increased intracellular $Ca^{2+}$ content, an effect that was inhibited by the extracellular $Ca^{2+}$ chelator ethylene glycol tetraacetic acid (EGTA) and the inositol 1,4,5-trisphosphate (IP3)-induced $Ca^{2+}$ release inhibitor 2-aminoethoxydiphenyl borate (2-APB). Further study showed that EGTA almost completely blocked Ang II-induced lysosome fusion, the translocation of acid sphingomyelinase (ASMase) to LR clusters, ASMase activation and NADPH (nicotinamide adenine dinucleotide phosphate) oxidase activation. In contrast, 2-APB had a slight inhibitory effect. Functionally, both the lysosome inhibitor bafilomycin A1 and the ASMase inhibitor amitriptyline reversed Ang II-induced impairment of vasodilation. We conclude that $Ca^{2+}$-regulated lysosome fusion mediates the Ang II-induced regulation of the LR-redox signaling pathway and mesenteric endothelial dysfunction.**
*Hypertension Research* (2016) **39,** 227–236; doi:10.1038/hr.2015.144; published online 14 January 2016

**Keywords:** arterial endothelium; molecular trafficking; vesicle fusion

## INTRODUCTION

Angiotensin (Ang) II has a critical role in the development of endothelial dysfunction and structural alterations (vascular remodeling) in small resistance arteries, mainly via the increased generation of reactive oxygen species driven by NADPH (nicotinamide adenine dinucleotide phosphate) oxidase activation.[1] It has been demonstrated that increased NADPH oxidase expression is involved in endothelial dysfunction and related vascular remodeling in model systems such as Ang II-induced hypertension in rats and mice.[2–5] Ang II also stimulates acute NADPH oxidase activation without changing the expression and levels of NADPH oxidase subunits. For example, Ang II acutely increased NADPH oxidase activity via the Ang II type 1 receptor (AT1R) and contributed to epithelial $Na^+$ channel activation in the cortical collecting duct of rats.[6] In isolated ventricular cardiac myocytes, Ang II activates $Ca^{2+}$/calmodulin-dependent protein kinase II via NADPH oxidase 2, resulting in the enhancement of diastolic sarcoplasmic reticulum $Ca^{2+}$ leakage.[7] In a kidney cell line, Ang II induces $Ca^{2+}$-dependent NADPH oxidase activation, leading to DNA damage.[8] Amiya *et al.*[9] reported that Ang II-induced acute reactive oxygen species production results directly in the deterioration of endothelial nitric oxide (NO) synthase $Ser^{1177}$ phosphorylation as well as NO production in rat aortic endothelial cells. A mechanistic study has revealed that Ang II activates NADPH oxidase via a protein kinase C-dependent pathway.[10] However, the mechanism underlying the acute activation of NADPH oxidase remains largely unknown.

Lipid rafts (LRs) are subdomains of the plasma membrane, which were initially identified by their resistance to Triton X-100 extraction.[11,12] Unlike the rest of the membrane, LRs are enriched in cholesterol and contain saturated acyl chains such as sphingolipids and glycosphingolipids.[13,14] Previously, we reported that lysosome trafficking and fusion to plasma membrane are crucial mechanisms in initiating LR clustering upon FasL (Fas ligand) and TRAIL (tumor necrosis factor-related apoptosis-inducing ligand) stimulation of coronary arterial endothelial cells. During lysosome fusion, lysosomal acid sphingomyelinase (ASMase) is translocated to the membrane and activated.[15–17] The product of ASMase (ceramide) then triggers the clustering of LRs and subunits of NADPH oxidase, including $gp91^{phox}$ and $p22^{phox}$, leading to the activation of this enzyme.[18–20] This signaling pathway represents the initial pathological change in coronary endothelial cells and can eventually lead to coronary atherosclerosis.[20,21]

Regulatory lysosomal exocytosis is an emergency response used to repair a ruptured plasma membrane[22–24] that is mediated by extracellular $Ca^{2+}$ influx in human fibroblasts,[25] epithelial cells[25] and

[1]State Key Laboratory of Medical Genetics, Shanghai Key Laboratory of Hypertension, Department of Hypertension, Ruijin Hospital, Shanghai Jiao Tong University School of Medicine, Shanghai, China; [2]Laboratory of Vascular Biology, Institute of Health Sciences, Shanghai Institutes for Biological Sciences, Chinese Academy of Sciences, Shanghai, China and [3]Shanghai Institute of Hypertension, Shanghai, China
Correspondence: Professor P-J Gao, Shanghai Institute of Hypertension, Ruijin Hospital, Shanghai Jiao Tong University School of Medicine, 197 Ruijin 2nd Road, Shanghai 200025, China.
E-mail: gaopingjin@sibs.ac.cn
Received 22 April 2015; revised 12 October 2015; accepted 19 October 2015; published online 14 January 2016

human keratinocytes.[26,27] Considering the critical role played by lysosome fusion in the LR-redox pathway, the Ang II-mediated increase of intracellular $Ca^{2+}$ in endothelial cells,[28–30] which in turn could lead to lysosome fusion. Thus, we hypothesized that Ang II induces the formation of an LR-redox signaling pathway and contributes to endothelial dysfunction in mesenteric arteries.

## METHODS

### Cell culture

Mesenteric endothelial cells (MECs) were harvested using a previously described method with slight modification.[31,32] Initially, the mesenteric arterial bed was isolated from Sprague-Dawley rats and perfused with Krebs solution containing (mmol $l^{-1}$) NaCl (118), KCl (4.7), $MgSO_4$ (1.2), $CaCl_2$ (2.5), $KH_2PO_4$ (1.2), $NaHCO_3$ (25) and glucose (11) bubbled with 95% $O_2$/5% $CO_2$ at 37 °C (pH: 7.4) at a flow rate of 1.0 ml $min^{-1}$ for 15 min to ensure thorough removal of the blood. The mesenteric arterial bed was then perfused with Krebs solution containing 0.2% type I collagenase (Worthington Biochemical, Lakewood, NJ, USA) at a flow rate of 2.0 ml $min^{-1}$ for 90 min. The perfusate collected during the first 30 min was discarded, after which the perfusate was collected every 10 min for 60 min and centrifuged at 1000 *g* for 10 min. The cells were resuspended in RPMI media containing 20% fetal bovine serum (Gibco, Life Technologies, Carlsbad, CA, USA) and 1% of a 100× antibiotic/antimycotic solution (Sigma, St Louis, MO, USA), then plated onto a six-well plate and incubated at 37 °C in 5% $CO_2$. After the cells reached confluence, they were passaged using trypsin-EDTA (Sigma) and plated on 100-mm-diameter cell culture dishes.

### Confocal analysis of LR clusters and their colocalization with ASMase

MECs were treated with Ang II for 20 min at the indicated concentration in the presence or absence of the AT1R inhibitor losartan (1 μmol $l^{-1}$, Sigma);[28] 1,2-Bis (2-aminophenoxy) ethane-N,N,N′,N′-tetraacetic acid tetrakis (acetoxymethyl ester; BAPTA-AM, 80 μg $ml^{-1}$, Sigma),[33] an intracellular $Ca^{2+}$ chelator; EGTA (5 mmol $l^{-1}$),[34] an extracellular $Ca^{2+}$ chelator; 2-aminoethoxydiphenyl borate (2-APB, 33 μmol $l^{-1}$),[29] a membrane permeable blocker of inositol 1,4,5-trisphosphate (IP3)-induced $Ca^{2+}$ release; the lysosome inhibitor bafilomycin A1 (100 nmol $l^{-1}$, Sigma); or the ASMase inhibitor amitriptyline (20 μmol $l^{-1}$, Sigma).[35] The detection of LRs was performed as previously described.[18–20] In brief, monosialotetrahexosylganglioside (GM1) in LRs was stained using Alexa 488-labeled cholera toxin B (Alexa 488-CTXB 1 μg $ml^{-1}$, 2 h, Molecular Probes, Eugene, CA, USA). Staining was visualized through sequential scanning on a confocal laser-scanning apparatus (Zeiss LSM510, Maple Grove, MN, USA) equipped with a ×60 objective. The majority of resting cells displayed a homogeneous distribution of fluorescence throughout the membrane and were marked as negative; clustering was defined as one or more intense spots or patches in each cell. The results were given as the percentage of cells containing one or more clusters after the indicated treatment.

To detect the colocalization of LRs and ASMase, MECs were further incubated with rabbit anti-ASMase polyclonal antibodies (1:500; Abcam, Cambridge, MA, USA) or mouse anti-gp91$^{phox}$ monoclonal antibody (1:250; BD Biosciences, San Jose, CA, USA) followed by incubation with Alexa fluor 555-conjugated anti-rabbit or anti-mouse secondary antibody (Molecular Probes, Carlsbad, CA, USA), respectively. Colocalization was analyzed using the Image Pro Plus software (Rockville, MD, USA), and the colocalization coefficient was represented by Pearson's correlation coefficient.[36]

### Intracellular $Ca^{2+}$ measurement

Confocal $Ca^{2+}$ imaging was employed to detect the real-time alteration in the intracellular $Ca^{2+}$ level.[37] In brief, MECs were treated with 0.1 μmol $l^{-1}$ Ang II in the presence or absence of losartan (1 μmol $l^{-1}$), EGTA (5 mmol $l^{-1}$), 2-APB (33 μmol $l^{-1}$) or xestospongin C (1 μmol $l^{-1}$).[38] MECs were incubated with 5 μmol $l^{-1}$ fluo-3-acetoxymethyl ester (fluo-3 AM) in the dark for 40 min and then washed for 20 min. Next, fluo-3 AM-loaded cells were allowed to settle on a confocal laser-scanning apparatus (Zeiss LSM510). Fluo-3 fluorescence was excited using the 488-nm line of an argon laser; and a fluorescence emitted at 510 nm was detected. All fluorescence measurements are expressed in arbitrary units generated from a pixel gray scale.

### FM1-43 quenching

FM1-43 quenching experiments were performed to detect lysosomal fusion to the cell membrane in MECs as described previously.[20] MEC lysosomes were loaded with 8 μmol $l^{-1}$ *N*-(3-triethylammoniumpropyl)-4-[4-(dibutylamino) styryl] pyridinium dibromide (FM1-43, Molecular Probes) for 2 h. Then, 1 mmol $l^{-1}$ bromide phenol blue (BPB) was added to the extracellular medium. FM1-43 fluorescence was monitored under confocal microscopy (Zeiss LSM510) with a low power laser (λ excitation = 488 nm). When lysosomes fuse to the cell membrane, BPB enters the cell and lysosomes to quench FM1-43 fluorescence. If there is no lysosome fusion, then FM1-43 fluorescence quenching does not occur.

### Flotation of membrane raft fractions

Detergent-resistant membrane fraction flotation was used to evaluate membrane raft clustering in MECs, as reported previously.[20] In brief, MECs were homogenized by five passages through a 25-gauge needle in lysis buffer. Homogenates were layered onto a step gradient consisting of 40, 30 and 5% OptiPrep Density Gradient medium. Then, the samples were centrifuged at 32 000 r.p.m. for 30 h at 4 °C in a SW32.1 rotor. The fractions were collected from top to bottom. After the addition of an equal volume of 30% trichloroacetic acid, the precipitated proteins were spun down by centrifugation at 13 000 r.p.m. at 4 °C for 15 min. The protein pellet was carefully washed with cold acetone and then used for immunoblot analysis.

### Assay of ASMase activity

The activity of ASMase was measured as described previously.[39] Briefly, cell homogenates (20 μg) were incubated with 0.02 μCi of *N*-methyl-[$^{14}$C]-sphingomyelin in 100 μl acidic reaction buffer containing 100 mmol $l^{-1}$ sodium acetate and 0.1% Triton X-100, pH 5.0, at 37 °C for 15 min. The reaction was terminated with 1.5 ml of a 2:1 chloroform:methanol solution and 0.2 ml double-distilled water. After vortexing and centrifuging at 1000 *g* for 5 min to separate the two phases, the upper aqueous phase containing the *N*-methyl-[$^{14}$C]-sphingomyelin metabolite $^{14}$C-choline phosphate was measured in a Beckman liquid scintillation counter. The choline phosphate

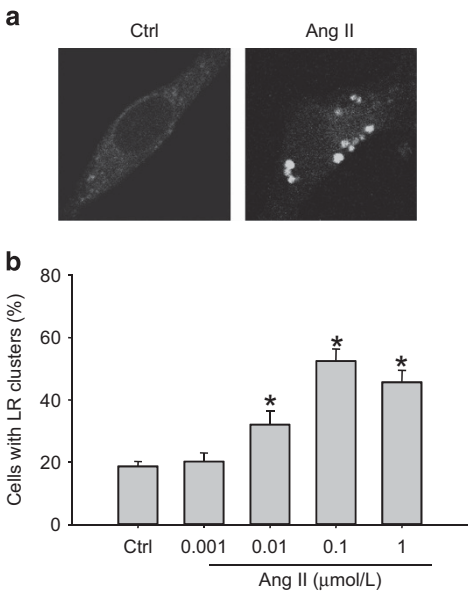


**Figure 1** Representative confocal fluorescence images (**a**) and summarized data (**b**) showing the effect of Ang II on LR formation in MECs. $n = 5–6$ batches of cells, $^*P < 0.05$ *vs.* a control group. A full color version of this figure is available at the *Hypertension Research* journal online.

formation rate was calculated to represent the enzyme activity.

### Lucigenin detection of endothelial $O_2^{\cdot -}$

Superoxide production in MECs was measured via lucigenin chemiluminescence as described previously.[40,41] Briefly, cells were incubated in vials containing 5 μmol l$^{-1}$ lucigenin (Sigma), and the NADPH oxidase activity was measured by lucigenin assay after the addition of NADPH (300 μmol l$^{-1}$). The light reaction between superoxide and lucigenin was detected using a chemiluminescence reader (BLR-201, Aloka, Wallingford, CT, USA).

### Endothelium-dependent vasodilation in isolated rat mesenteric artery

Segments of third-order branches of the mesenteric artery were mounted in a Multi Myograph 610 M (DMT, Aarhus, Denmark) for isometric tension recording as described previously.[42,43] Thirty minutes after the resting tension was established, mesenteric resistance arteries were maximally contracted using a $K^+$-depolarizing solution of the following composition (in mmol l$^{-1}$): NaCl (16.7), KCl (100), $KH_2PO_4$ (1.2), $MgSO_4$ (1.2), $CaCl_2$ (2.5), glucose (11.1) and $NaHCO_3$ (25). In endothelium-intact rings, acetylcholine at 1 mmol l$^{-1}$ typically resulted in ⩾80% relaxation, and removal of the endothelium was confirmed by a lack of relaxation in response to acetylcholine. Responses to acetylcholine ($10^{-10}$–$10^{-6}$ mol l$^{-1}$) were obtained in arteries precontracted with phenylephrine (10 μmol l$^{-1}$) after a 30-min incubation with bafilomycin A1 (100 nmol l$^{-1}$, Sigma), amitriptyline (20 μmol l$^{-1}$, Sigma) or the specific NADPH oxidase inhibitor apocynin (100 μmol l$^{-1}$)[44] with or without 0.1 μmol l$^{-1}$ Ang II. Tension was recorded using a high-sensitivity isometric force transducer, and was stored using the Chart version 5.4.1 software program (Powerlab, AD Instruments, Bella Vista, NSW, Australia) until further analysis.

### Statistics

Data are presented as the mean ± s.e. Significant differences between and within multiple groups were examined using ANOVA for repeated measures, followed by Duncan's multiple-range test. A Student's *t*-test was used to detect significant differences between two groups. $P<0.05$ was considered as statistically significant.

## RESULTS

### Effect of Ang II on LR formation in MECs

The effect of Ang II on LR clustering in MECs was evaluated by staining for ganglioside GM1 using a specific marker CTXB subunit. We found that LRs were diffusely distributed across the cell membrane under control conditions as indicated by weak, diffuse green fluorescence (Figure 1a). Upon stimulation with Ang II at

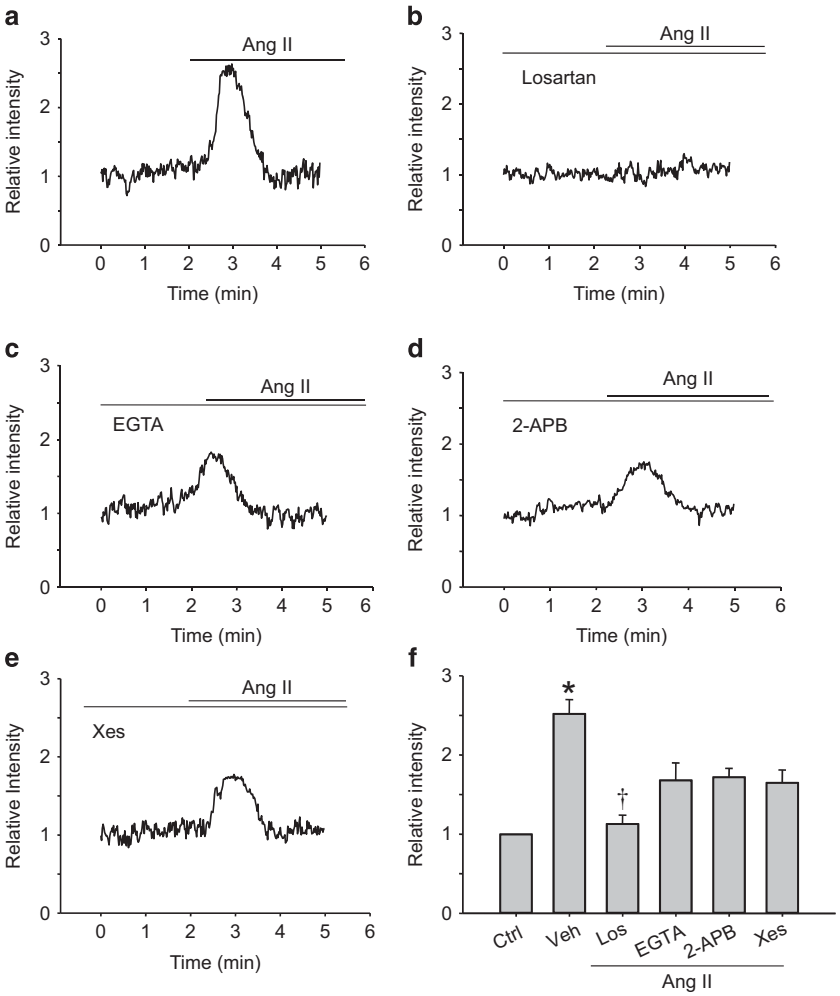


**Figure 2** Representative graphic representation (**a**–**e**) and summarized data (**f**) showing the effect of losartan, BAPTA-AM, EGTA, 2-APB and xestospongin C on Ang II-induced $Ca^{2+}$ increase in MECs. Cultured MECs were loaded with fluo-3 AM, and 0.1 μmol l$^{-1}$ Ang II was added to trigger an increase in intracellular $Ca^{2+}$ (i.e., fluorescence level) with or without pretreatment with losartan, BAPTA-AM, EGTA, 2-APB or xestospongin C. Four to six cells were examined in each experiment (one plate of cells was used); $n=5$ independent experiments. *$P<0.05$ *vs.* other groups; †$P<0.05$ *vs.* EGTA, 2-APB or xestospongin C groups. Ctrl, control; Los, losartan; Veh, vehicle; Xes, xestospongin C.

0.1 μmol l$^{-1}$ for 20 min, clustering of LR occurred, as indicated by the formation of brighter patches of green fluorescence. The data in Figure 1b show that only a small percentage of the resting cells exhibited these clusters (18.7%), and Ang II increased LR clustering in MECs in a dose-dependent manner.

### Ang II stimulates intracellular $Ca^{2+}$ increase in MECs

Next, we evaluated whether Ang II elicits an intracellular $Ca^{2+}$ increase. Figure 2 demonstrates that the application of Ang II at 0.1 μmol l$^{-1}$ quickly increased intracellular $Ca^{2+}$ in a fluo-3 AM assay, and that this effect was significantly inhibited by the AT1R inhibitor losartan. We next examined whether extracellular $Ca^{2+}$ influx and intracellular $Ca^{2+}$ release were involved in this process. As shown in Figure 2, Ang II-induced intracellular $Ca^{2+}$ increase was partially inhibited by the extracellular $Ca^{2+}$ chelator EGTA, as well as the unspecific and specific IP3-dependent intracellular $Ca^{2+}$ release blockers 2-APB and xestospongin C, respectively. These results indicate that Ang II elicits an intracellular $Ca^{2+}$ increase via AT1R-mediated extracellular $Ca^{2+}$ influx and IP3-dependent intracellular $Ca^{2+}$ release.

### Involvement of intracellular $Ca^{2+}$ increase in Ang II-stimulated lysosome fusion

We next examined whether this intracellular $Ca^{2+}$ increase has a role in Ang II-induced lysosome fusion via a lysosomal dye FM1-43 quenching assay. MECs were incubated with FM1-43 for 2 h to preload lysosomes, and then BPB was added, followed immediately by treatment with Ang II. Lysosome fusion was detected by a decrease in FM1-43 fluorescence after Ang II treatment, due to release of the dye into the external medium, followed by quenching with BPB, a membrane-impermeable quencher. Therefore, FM1-43 fluorescence quenching indicates lysosome fusion. Under control (that is, unstimulated) conditions, FM1-43-loaded MECs exhibited sustained fluorescence over a 30-min period (data not shown). When the cells were stimulated with Ang II, a marked reduction of fluorescence intensity occurred over the same time period, as shown by confocal fluorescence imaging and by continuous recording of changes in fluorescence intensity in the lysosomes of MECs (Figure 3a). In such recordings, each curve represents a fluorescence change in one MEC lysosome. When these cells were pretreated with BAPTA-AM or EGTA, Ang II-induced quenching was almost fully blocked. In contrast, the stimulatory effect of Ang II was slightly attenuated by 2-APB (Figure 3b). These results indicate that extracellular $Ca^{2+}$ influx may have a major role in Ang II-induced lysosome fusion, although IP3-dependent intracellular $Ca^{2+}$ release might also be involved.

### Involvement of $Ca^{2+}$-mediated lysosome fusion in Ang II-induced LR formation, ASMase translocation and activation

Previous studies have shown that lysosome fusion results in ASMase activation and LR formation. We therefore evaluated whether Ang II-induced $Ca^{2+}$-regulated lysosome fusion mediates LR formation. As shown in Figure 4a, Ang II induced significant LR formation that was almost fully blocked by losartan, BAPTA-AM and EGTA. Figure 4b shows that ASMase was translocated to the plasma membrane; and its colocalization with LRs increased in response to Ang II stimulation. The summarized data in Figures 4c and 5 demonstrate that Ang II-induced colocalization of LRs with ASMase, and ASMase activation observed via $^{14}$C-choline phosphate assay was almost fully blocked by losartan, BAPTA-AM and EGTA. In contrast, 2-APB yielded only slight inhibitory effects (Figures 4 and 5c). These results indicate that $Ca^{2+}$-mediated lysosome fusion via AT1R has a major role in Ang II-induced ASMase translocation, activation and subsequent LR formation in MECs.

The effect of Ang II on LR formation was evaluated using a detergent-resistant membrane fraction flotation assay. As shown in Figures 5a and b, flotillin-1, a membrane-raft-specific marker, was primarily found in the fractions between the 5 and 30% gradients (2–4). In control cells, the specific lysosome marker lysosome-

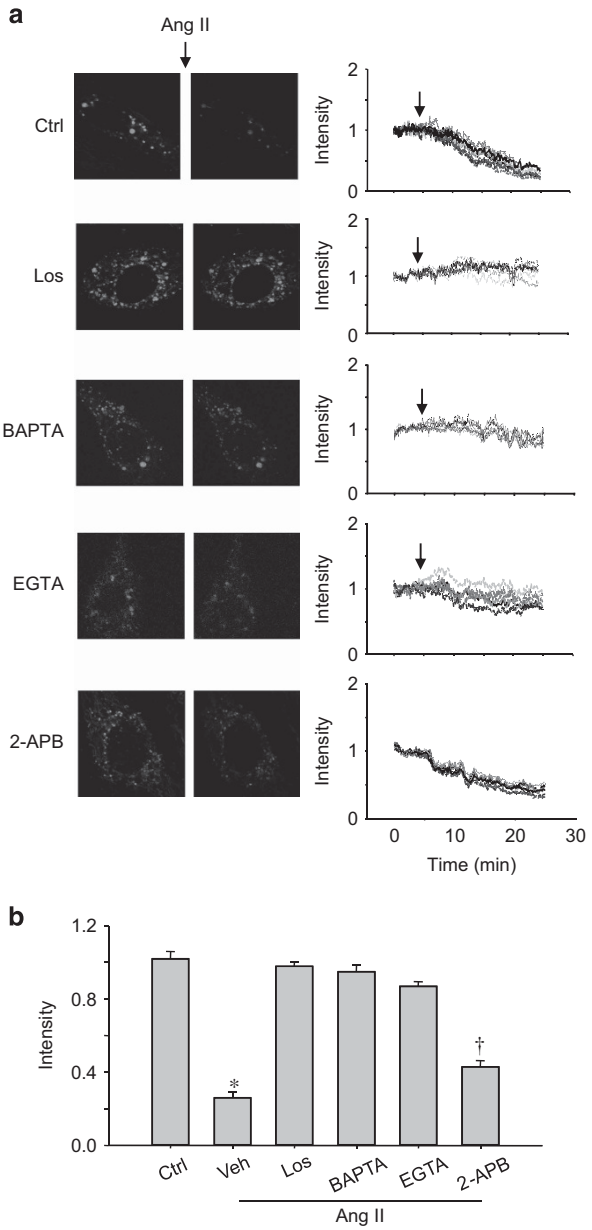


**Figure 3** The involvement of intracellular $Ca^{2+}$ in Ang II-induced lysosomal fusion. (**a**) Representative confocal microscopic images (left) and fluorescence traces (right), and summarized data (**b**) showing inhibition by losartan, BAPTA-AM, EGTA or 2-APB of Ang II-induced quenching of FM1-43 fluorescence in MECs. The cells were pre-loaded with FM1-43, and BPB was added immediately before Ang II treatment. The arrows indicate the onset of Ang II treatment. For each group, the change in fluorescence was normalized to the fluorescence intensity obtained immediately before Ang II treatment. $n=6$ batches of cells; $^*P<0.05$ *vs.* other groups; †$P<0.05$ *vs.* losartan, BAPTA or EGTA groups. Ctrl, control; Los, losartan; Veh, vehicle. A full color version of this figure is available at the *Hypertension Research* journal online.

associated membrane protein 1 (Lamp-1) was found primarily in the non-lipid-raft domain, and Ang II treatment caused a marked shift in the Lamp-1 distribution from a non-lipid-raft domain to the membrane raft domain (Figures 5a and b).

Previous studies have shown that ATRs are located in the plasma membrane LR domain and that their activity is closely related to LR activity. We therefore evaluated whether cholesterol (that is, an LR component) depletion affects Ang II-induced LR formation. We found that cholesterol depletion via MCD (methy-b-cyclodextrin) almost fully blocked Ang II-induced LR clustering (Control, 16.7 ± 1.6%; Ang II, 52.5 ± 3.8%; MCD+Ang II, 20.3 ± 2.4%. $P<0.05$ for the Ang II group *vs.* the two other groups).

### Involvement of $Ca^{2+}$-mediated lysosome fusion in Ang II-induced gp91$^{phox}$ clustering and $O_2^{\cdot -}$ production

We next evaluated whether Ang II-induced LR formation resulted in NADPH oxidase subunit gp91$^{phox}$ clustering and activation because previous studies have shown that NADPH oxidase subunits cluster

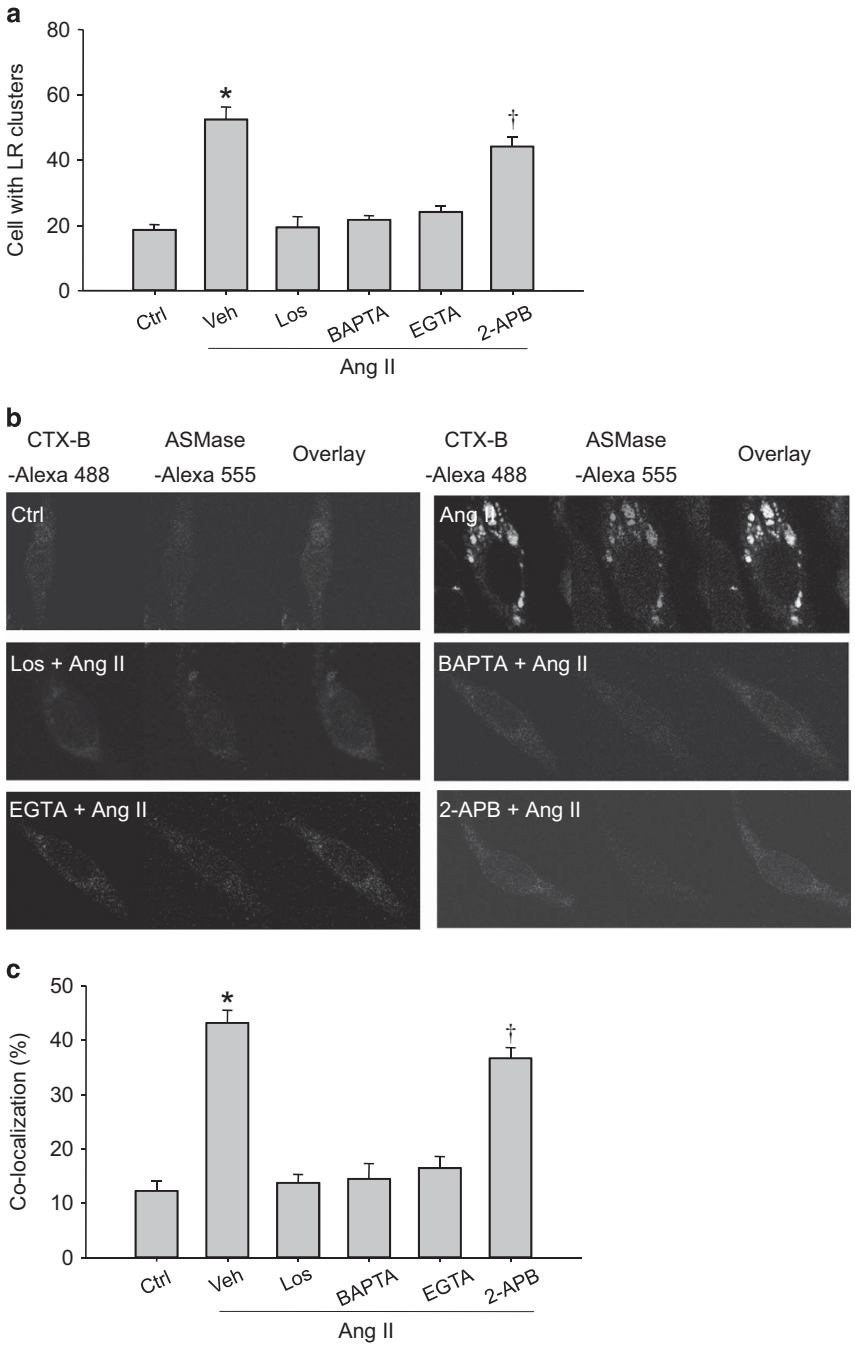


**Figure 4** The effects of intracellular $Ca^{2+}$-mediated lysosome fusion on Ang II LR formation and colocalization with ASMase. (**a**) The inhibitory effects of losartan, BAPTA-AM, EGTA and 2-APB on Ang II-induced LR formation in MECs. (**b**) Representative confocal fluorescence images and summarized data (**c**) for the inhibitory effects of losartan, BAPTA-AM and 2-APB on Ang II-induced colocalization between LRs and ASMase. $n=6$ batches of cells; *$P<0.05$ *vs.* other groups; †$P<0.05$ *vs.* losartan, BAPTA or EGTA groups. Ctrl, control; Los, losartan; Veh, vehicle. A full color version of this figure is available at the *Hypertension Research* journal online.

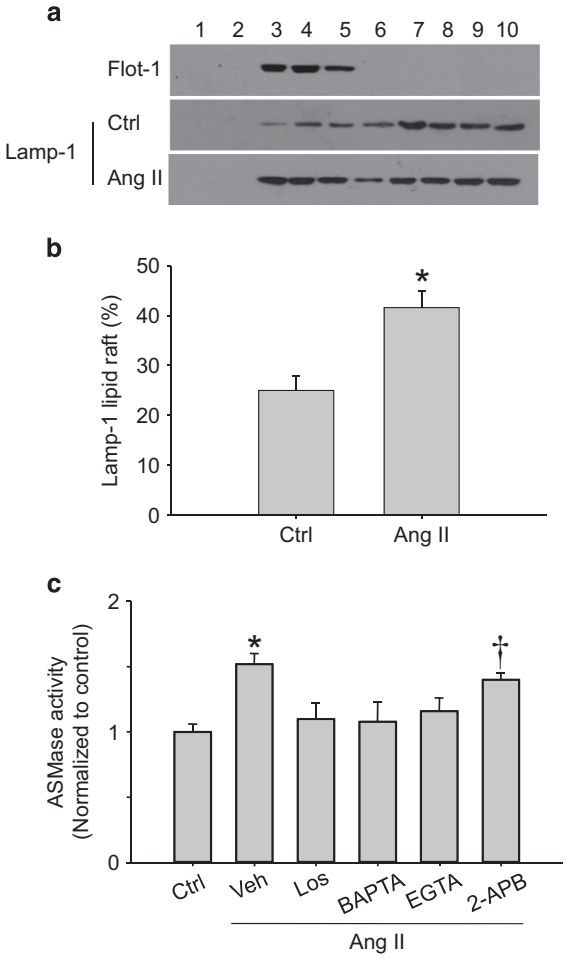


**Figure 5** Representative immunoblot figures (**a**) and summarized data (**b**) showing the effect of Ang II on Lamp-1 distribution in MECs. MECs treated with or without stimulation of Ang II for 20 min were subjected to immunoblot analysis of either flotillin-1 (flot-1) or Lamp-1. The numbers (1–10) at top indicate the membrane fractions isolated by gradient centrifugation from top to bottom. Fractions 1–2 were very light and without proteins. Fractions 3–5 were light fractions designated as membrane rafts based on the presence of the LR marker protein flot-1. The heavier fractions 6–10 were designated as non-raft fractions and contained membrane and cytosolic proteins. (**c**) A bar graph showing the inhibitory effects of losartan, BAPTA-AM, EGTA and 2-APB on Ang II-induced ASMase activation. ASMase activity was measured by the quantification of choline phosphate production using radiometry. $n=5$–6 batches of cells; $^*P<0.05$ *vs.* control group; $\dagger P<0.05$ *vs.* vehicle group; $\dagger P<0.05$ *vs.* losartan, BAPTA or EGTA groups. Ctrl, control; Los, losartan; Veh, vehicle. A full color version of this figure is available at the *Hypertension Research* journal online.

upon LR clustering. As shown in Figure 6, Ang II treatment for 20 min induced significant LR formation and gp91$^{phox}$ clustering. Similarly, Ang II stimulated acute $O_2^{\cdot -}$ production in MECs, as measured by lucigenin assay; this increase was almost fully blocked by losartan, BAPTA-AM, EGTA, the lysosome inhibitor bafilomycin A1 and the specific lysosome fusion inhibitor tetanus toxin. As expected, the ASMase inhibitor amitriptyline also effectively blocked Ang II-induced LR formation, gp91$^{phox}$ clustering and $O_2^{\cdot -}$ production. In contrast, 2-APB showed only a slight inhibitory effect (Figure 7a). These results indicate that Ang II acutely activates the LR-redox signaling pathway via $Ca^{2+}$-mediated lysosome fusion and ASMase activation.

### Involvement of $Ca^{2+}$-mediated lysosome fusion in Ang II-induced impairment of endothelium-dependent vasodilation

Finally, the effect of the Ang II-induced LR-redox signaling pathway on vascular function was determined using isolated mesenteric artery segments. The arteries were first treated with Ang II with or without bafilomycin A1, amitriptyline or the NADPH oxidase inhibitor apocynin; and then the effects of dose-dependent vasodilation using acetylcholine were examined. Figure 7b shows that the addition of Ang II significantly attenuated acetylcholine-induced vasodilation. In the presence of bafilomycin A1 or amitriptyline, the inhibitory effect of Ang II on acetylcholine-induced vasodilation was significantly reversed. Furthermore, Ang II-induced impairment of vasodilation was significantly inhibited by apocynin. These findings indicate that Ang II induced the impairment of vasodilation, at least in part through the activation of the LR-redox signaling pathway upon lysosome fusion via ASMase.

## DISCUSSION

In the present study, we report that Ang II activates NADPH oxidase through the formation of LRs in mesenteric arterial endothelial cells. Mechanistic experiments revealed that Ang II elicits an intracellular $Ca^{2+}$ increase in response to AT1R-mediated extracellular $Ca^{2+}$ influx and IP3-dependent intracellular $Ca^{2+}$ release. Furthermore, extracellular $Ca^{2+}$-mediated lysosome fusion has a major role in Ang II-induced translocation of lysosomal ASMase to the plasma membrane, thereby leading to LR formation, NADPH oxidase subunit clustering, increased $O_2^{\cdot -}$ production and the impairment of vasodilation in mesenteric arteries. This signaling pathway may contribute to diseases involving endothelial dysfunction, such as hypertension.

We characterized the formation of LR clusters on the cell membrane of MECs using confocal microscopic analysis with CTX as a marker. CTX binds to the ganglioside GM1, which partitions into LRs, relatively specifically; thus, this method has been used extensively to evaluate LR clustering in endothelial cells in our previous studies[20] as well as by other laboratories.[45] Furthermore, we found that this effect was mediated by AT1R. Indeed, the AT1 receptor has a critical role in Ang II-mediated actions in the cardiovascular system, including vasoconstriction, hypertrophy, proliferation, fibrosis and oxidative stress, while the functions of the AT2R tend to oppose those of the AT1R.[2]

Previous studies have shown that AT1R activation increases intracellular $Ca^{2+}$ and initiates various signaling pathways in endothelial cells, podocytes, rat carotid body type II cells and cardiac fibroblasts.[28,30,46–48] Furthermore, both extracellular $Ca^{2+}$ influx and intracellular $Ca^{2+}$ release have been shown to mediate Ang II-induced intracellular $Ca^{2+}$ increase.[30,46–48] For example, it has been shown that AT1R-mediated extracellular $Ca^{2+}$ influx mediates Ang II-induced vasocontraction in vascular smooth muscle cells in the rat aorta;[49] whereas AT1R-mediated intracellular $Ca^{2+}$ release mediates collagen synthesis in cardiac fibroblasts[47] and activates pannexin-1 channels in rat carotid body type II cells.[46] Importantly, $Ca^{2+}$-regulated exocytosis of lysosomes is of great importance for acquiring new plasma membrane components to repair wounded cells with torn plasma membranes, a critical function in cells that are frequently mechanically stressed.[26] Indeed, inomycin, an effective $Ca^{2+}$ ionopohre commonly used to increase intracellular $Ca^{2+}$ concentration, has been used extensively to investigate the mechanisms underlying lysosome fusion. It has been shown that inomycin induces lysosome exocytosis, and is involved in membrane repair in human fibroblasts and epithelial cells[25] as well as in human keratinocytes.[26] These results are consistent

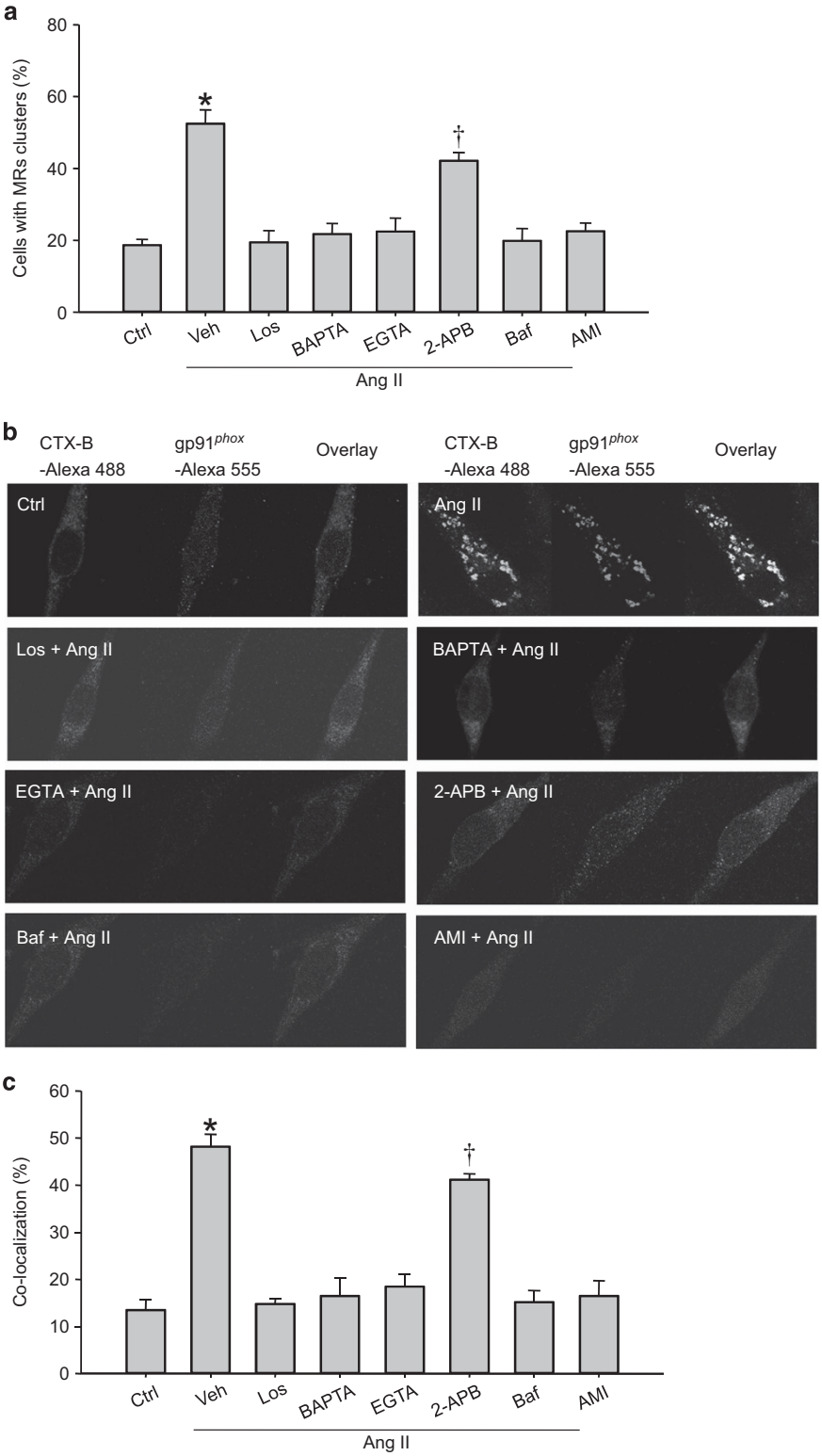


**Figure 6** The effects of intracellular $Ca^{2+}$-mediated lysosome fusion on Ang II LR formation and colocalization with $gp91^{phox}$. (**a**) The inhibitory effects of losartan, BAPTA-AM, EGTA, 2-APB, bafilomycin A1 and amitriptyline on Ang II-induced LR formation in MECs. (**b**) Representative confocal fluorescence images and summarized data (**c**) for the inhibitory effects of losartan, BAPTA-AM, EGTA, 2-APB, bafilomycin A1 and amitriptyline on Ang II-induced colocalization of LRs and $gp91^{phox}$. $n=6$ batches of cells; $*P<0.05$ *vs.* other groups; $\dagger P<0.05$ *vs.* losartan, BAPTA, EGTA, bafilomycin A1 or amitriptyline groups. AMI, amitriptyline; Baf, bafilomycin A1; Ctrl, control; Los, losartan; Veh, vehicle. A full color version of this figure is available at the *Hypertension Research* journal online.

with the present study, which shows that extracellular $Ca^{2+}$ has a major role in Ang II-induced lysosome fusion. In addition, IP3-dependent intracellular $Ca^{2+}$ release is involved in Ang II-induced lysosome fusion, consistent with previous studies showing that intracellular $Ca^{2+}$ release is sufficient for the secretory response, including lysosome fusion.[50] It is likely that extracellular $Ca^{2+}$ elicits the fusion of most potential lysosomes with the plasma membrane, whereas intracellular $Ca^{2+}$ release can only stimulate the fusion of a portion of all lysosomes to fuse with plasma membrane.

We have demonstrated that lysosomal ASMase translocates to the plasma membrane and is activated upon lysosome fusion in response to FasL and TRAIL stimulation.[21,51–54] The early product of AMSase ceramide may initiate the activation of lysosome trafficking and fusion with the cell membrane, resulting in the production a large amount of ceramide, which then triggers LR clustering.[18] Consistent with these studies, the present study shows that Ang II significantly increased LR formation and colocalization with ASMase as well as ASMase activity, as shown by $^{14}$C-choline phosphate assay. Importantly, the translocation and activation of ASMase are mediated by lysosome fusion, because the Ang II-induced effects were lost when lysosome fusion was inhibited by the AT1R inhibitors losartan, BAPTA-AM, EGTA and 2-APB, consistent with previous studies showing that lysosome fusion results in ASMase translocation and the activation coronary arterial endothelial cells in response to FasL stimulation. The finding that Ang II increased the translocation of Lamp-1 from non-LRs to LRs domain suggests that the lysosome is involved in the Ang II-induced effect in MECs. Furthermore, it has been reported that extracellular $Ca^{2+}$ influx induces ASMase activation in NRK cells and mediates membrane repair following damage, although the mechanisms involved remain unknown.[55] Previous studies have shown that ATRs are located in the plasma membrane LR domain, and that their activity is closely related to the LR.[56,57] Consistent with these findings, the present study shows that cholesterol depletion by MCD almost fully blocked Ang II-induced LR clustering. However, this inhibitory effect could be caused by the inhibition of AT1R activity or the direct inhibition of LR formation. In light of the finding that Ang II-induced LR formation is effectively inhibited by the lysosome function inhibitor bafilomycin A1 and the ASMase inhibitor amitriptyline, we conclude that Ang II induces LR formation in a lysosome-dependent manner.

The acute effect of Ang II on NADPH oxidase activation has been documented in various cell types.[6–8] Our previous studies show that NADPH oxidase subunits cluster together as a consequence of LR clustering, resulting in increased NADPH oxidase activity.[17,20] Consistent with these findings, the present study shows that Ang II significantly increased NADPH oxidase subunit gp91$^{phox}$ clustering and NADPH oxidase activity. Importantly, these effects were mediated by Ang II-induced lysosome fusion and subsequent ASMase activation, because the stimulatory effect of Ang II was attenuated when lysosome fusion was inhibited by losartan; BAPTA-AM; EGTA and 2-APB; bafilomycin A1; or amitriptyline. The involvement of the LR-redox signaling pathway was further confirmed by the finding that the use of bafilomycin A1 or amitriptyline effectively blocked Ang II-induced impairment of vasodilation. The present finding that Ang II activates NADPH oxidase via LR signaling pathway is in conflict with a previous study showing that Ang II activated NADPH oxidase via a PKC-dependent pathway in cardiac myocytes,[10] indicating that Ang II may acutely activate NADPH oxidase via various signaling pathways in different cell types.

In contrast to our finding that Ang II acutely induces reactive oxygen species production in MECs, Pueyo *et al.*[28] reported that Ang II induces NO production in rat aortic endothelial cells and in vascular smooth muscle cells.[58] These results indicate that Ang II may have a dual effect on vascular endothelial cells. Extracellular $Ca^{2+}$ influx activation of the LR-redox signaling pathway may be the result of membrane proximal lysosome fusion with the plasma membrane in MECs, because membrane proximal lysosomes are the vesicles primarily responsible for $Ca^{2+}$ influx-dependent exocytosis,[59] although intracellular $Ca^{2+}$ release is also partially involved. In contrast, Ang II-induced NO production may involve intracellular $Ca^{2+}$ release, thereby leading to the activation of NO synthase, which is known to be the mechanism underlying the function of the well-known vasodilators acetylcholine[60,61] and bradykinin.[62] Indeed, the effect of chronic infusion of Ang II on endothelial function has been documented previously.[63,64] The present finding that Ang II acutely activates an LR-redox signaling pathway may represent an early stage of endothelial dysfunction in Ang II-induced hypertension.

In summary, the present study demonstrated that diffuse LR components were clustered in mesenteric arterial endothelial cells and that NADPH oxidase was activated in response to Ang II activation. This novel transmembrane signaling mechanism may contribute to the regulation of endothelial function under different physiological and pathological conditions.

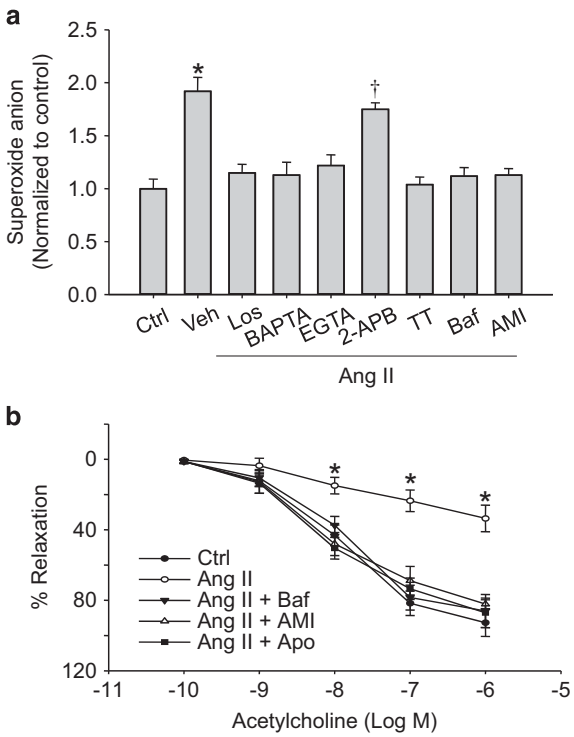


**Figure 7** (**a**) Summarized data showing the inhibitory effects of losartan, BAPTA-AM, EGTA, 2-APB, tetanus toxin, the lysosome inhibitor bafilomycin A1 and the ASMase inhibitor amitriptyline on Ang II-induced $O_2^{\cdot-}$ production in MECs using a lucigenin assay. $n=4$–6 batches of cells, $^*P<0.05$ *vs.* control group, $^\dagger P<0.05$ *vs.* vehicle group. (**b**) Bafilomycin A1, amitriptyline and apocynin blocked Ang II-induced (0.1 μmol l$^{-1}$ for 30 min) damage of the vasodilator response. $n=5$ rats. $^*P<0.05$ *vs.* control, Ang II+bafilomycin A1, Ang II+amitriptyline or Ang II+apocynin groups. $^\dagger P<0.05$ *vs.* losartan, BAPTA, EGTA, tetanus toxin, bafilomycin A1 or amitriptyline groups. AMI, amitriptyline; Apo, apocynin; Baf, bafilomycin A1; Ctrl, control; Los, losartan; TT, tetanus toxin; Veh, vehicle.

## CONFLICT OF INTEREST

The authors declare no conflict of interest.

## ACKNOWLEDGEMENTS

This study was supported by the National Natural Science Foundation of China (81100184, 81230071, 81570221, 91539202, 81200203 and 81300089), the Pujiang Program of the Shanghai Science and Technology Committee (14PJ1406400), the Shanghai Medical Bureau Fund (201540037), the Scientific Fund of Shanghai Jiao Tong University School of Medicine (14XJ10042) and the Scientific Research Foundation for the Returned Overseas Chinese Scholars of the State Education Ministry.

1 Touyz RM. Reactive oxygen species as mediators of calcium signaling by angiotensin II: implications in vascular physiology and pathophysiology. *Antioxid Redox Signal* 2005; **7**: 1302–1314.
2 Ma TK, Kam KK, Yan BP, Lam YY. Renin-angiotensin-aldosterone system blockade for cardiovascular diseases: current status. *Br J Pharmacol* 2010; **160**: 1273–1292.
3 Harrison DG, Gongora MC. Oxidative stress and hypertension. *Med Clin North Am* 2009; **93**: 621–635.
4 Jung O, Schreiber JG, Geiger H, Pedrazzini T, Busse R, Brandes RP. gp91phox-containing NADPH oxidase mediates endothelial dysfunction in renovascular hypertension. *Circulation* 2004; **109**: 1795–1801.
5 Zhang H, Schmeisser A, Garlichs CD, Plotze K, Damme U, Mugge A, Daniel WG. Angiotensin II-induced superoxide anion generation in human vascular endothelial cells: role of membrane-bound NADH-/NADPH-oxidases. *Cardiovasc Res* 1999; **44**: 215–222.
6 Sun P, Yue P, Wang WH. Angiotensin II stimulates epithelial sodium channels in the cortical collecting duct of the rat kidney. *Am J Physiol Renal Physiol* 2012; **302**: F679–F687.
7 Wagner S, Dantz C, Flebbe H, Azizian A, Sag CM, Engels S, Mollencamp J, Dybkova N, Islam T, Shah AM, Maier LS. NADPH oxidase 2 mediates angiotensin II-dependent cellular arrhythmias via PKA and CaMKII. *J Mol Cell Cardiol* 2014; **75**: 206–215.
8 Fazeli G, Stopper H, Schinzel R, Ni CW, Jo H, Schupp N. Angiotensin II induces DNA damage via AT1 receptor and NADPH oxidase isoform Nox4. *Mutagenesis* 2012; **27**: 673–681.
9 Amiya E, Watanabe M, Takeda N, Saito T, Shiga T, Hosoya Y, Nakao T, Imai Y, Manabe I, Nagai R, Komuro I, Maemura K. Angiotensin II impairs endothelial nitric-oxide synthase bioavailability under free cholesterol-enriched conditions via intracellular free cholesterol-rich membrane microdomains. *J Biol Chem* 2013; **288**: 14497–14509.
10 White CN, Figtree GA, Liu CC, Garcia A, Hamilton EJ, Chia KK, Rasmussen HH. Angiotensin II inhibits the $Na^+$-$K^+$ pump via PKC-dependent activation of NADPH oxidase. *Am J Physiol Cell Physiol* 2009; **296**: C693–C700.
11 Lang T. SNARE proteins and 'membrane rafts'. *J Physiol* 2007; **585**: 693–698.
12 Vetrivel KS, Thinakaran G. Membrane rafts in Alzheimer's disease beta-amyloid production. *Biochim Biophys Acta* 2010; **1801**: 860–867.
13 Liu J, Aoki M, Illa I, Wu C, Fardeau M, Angelini C, Serrano C, Urtizberea JA, Hentati F, Hamida MB, Bohlega S, Culper EJ, Amato AA, Bossie K, Oeltjen J, Bejaoui K, McKenna-Yasek D, Hosler BA, Schurr E, Arahata K, de Jong PJ, Brown RH Jr. Dysferlin, a novel skeletal muscle gene, is mutated in Miyoshi myopathy and limb girdle muscular dystrophy. *Nat Genet* 1998; **20**: 31–36.
14 Simons K, Ikonen E. Functional rafts in cell membranes. *Nature* 1997; **387**: 569–572.
15 Shao D, Segal AW, Dekker LV. Lipid rafts determine efficiency of NADPH oxidase activation in neutrophils. *FEBS Lett* 2003; **550**: 101–106.
16 Jin S, Zhang Y, Yi F, Li PL. Critical role of lipid raft redox signaling platforms in endostatin-induced coronary endothelial dysfunction. *Arterioscler Thromb Vasc Biol* 2008; **28**: 485–490.
17 Bao JX, Jin S, Zhang F, Wang ZC, Li N, Li PL. Activation of membrane NADPH oxidase associated with lysosome-targeted acid sphingomyelinase in coronary endothelial cells. *Antioxid Redox Signal* 2010; **12**: 703–712.
18 Han WQ, Xia M, Zhang C, Zhang F, Xu M, Li NJ, Li PL. SNARE-mediated rapid lysosome fusion in membrane raft clustering and dysfunction of bovine coronary arterial endothelium. *Am J Physiol Heart Circ Physiol* 2011; **301**: H2028–H2037.
19 Li X, Han WQ, Boini KM, Xia M, Zhang Y, Li PL. TRAIL death receptor 4 signaling via lysosome fusion and membrane raft clustering in coronary arterial endothelial cells: evidence from ASM knockout mice. *J Mol Med (Berl)* 2013; **91**: 25–36.
20 Han WQ, Xia M, Xu M, Boini KM, Ritter JK, Li NJ, Li PL. Lysosome fusion to the cell membrane is mediated by the dysferlin C2A domain in coronary arterial endothelial cells. *J Cell Sci* 2012; **125**: 1225–1234.
21 Zhang AY, Yi F, Zhang G, Gulbins E, Li PL. Lipid raft clustering and redox signaling platform formation in coronary arterial endothelial cells. *Hypertension* 2006; **47**: 74–80.
22 Andrews NW. Regulated secretion of conventional lysosomes. *Trends Cell Biol* 2000; **10**: 316–321.
23 Stinchcombe JC, Griffiths GM. Regulated secretion from hemopoietic cells. *J Cell Biol* 1999; **147**: 1–6.
24 Reddy A, Caler EV, Andrews NW. Plasma membrane repair is mediated by Ca($2^+$)-regulated exocytosis of lysosomes. *Cell* 2001; **106**: 157–169.
25 Rodriguez A, Webster P, Ortego J, Andrews NW. Lysosomes behave as $Ca^{2+}$-regulated exocytic vesicles in fibroblasts and epithelial cells. *J Cell Biol* 1997; **137**: 93–104.
26 Jans R, Sartor M, Jadot M, Poumay Y. Calcium entry into keratinocytes induces exocytosis of lysosomes. *Arch Dermatol Res* 2004; **296**: 30–41.
27 Holt OJ, Gallo F, Griffiths GM. Regulating secretory lysosomes. *J Biochem* 2006; **140**: 7–12.
28 Pueyo ME, Arnal JF, Rami J, Michel JB. Angiotensin II stimulates the production of NO and peroxynitrite in endothelial cells. *Am J Physiol* 1998; **274**: C214–C220.
29 Fellner SK, Arendshorst WJ. Angiotensin II $Ca^{2+}$ signaling in rat afferent arterioles: stimulation of cyclic ADP ribose and IP3 pathways. *Am J Physiol Renal Physiol* 2005; **288**: F785–F791.
30 Nitschke R, Henger A, Ricken S, Gloy J, Muller V, Greger R, Pavenstadt H. Angiotensin II increases the intracellular calcium activity in podocytes of the intact glomerulus. *Kidney Int* 2000; **57**: 41–49.
31 Santos CF, Caprio MA, Oliveira EB, Salgado MC, Schippers DN, Munzenmaier DH, Greene AS. Functional role, cellular source, and tissue distribution of rat elastase-2, an angiotensin II-forming enzyme. *Am J Physiol Heart Circ Physiol* 2003; **285**: H775–H783.
32 Gomez-Sanchez CE, Foecking MF, Ferris MW, Hieda HS, Gomez-Sanchez EP. Rat mesenteric artery endothelial cells in culture secrete ET-1. *Life Sci* 1990; **46**: 881–884.
33 Lioi AB, Rodriguez AL, Funderburg NT, Feng Z, Weinberg A, Sieg SF. Membrane damage and repair in primary monocytes exposed to human beta-defensin-3. *J Leukoc Biol* 2012; **92**: 1083–1091.
34 Menezes-Rodrigues FS, Pires-Oliveira M, Duarte T, Paredes-Gamero EJ, Chiavegatti T, Godinho RO. Calcium influx through L-type channels attenuates skeletal muscle contraction via inhibition of adenylyl cyclases. *Eur J Pharmacol* 2013; **720**: 326–334.
35 Bao JX, Xia M, Poklis JL, Han WQ, Brimson C, Li PL. Triggering role of acid sphingomyelinase in endothelial lysosome-membrane fusion and dysfunction in coronary arteries. *Am J Physiol Heart Circ Physiol* 2010; **298**: H992–H1002.
36 Zinchuk V, Zinchuk O, Okada T. Quantitative colocalization analysis of multicolor confocal immunofluorescence microscopy images: pushing pixels to explore biological phenomena. *Acta Histochem Cytochem* 2007; **40**: 101–111.
37 Han WQ, Zhu DL, Wu LY, Chen QZ, Guo SJ, Gao PJ. N-acetylcysteine-induced vasodilation involves voltage-gated potassium channels in rat aorta. *Life Sci* 2009; **84**: 732–737.
38 Elamin E, Masclee A, Dekker J, Jonkers D. Ethanol disrupts intestinal epithelial tight junction integrity through intracellular calcium-mediated Rho/ROCK activation. *Am J Physiol Gastrointest Liver Physiol* 2014; **306**: G677–G685.
39 Liu B, Hannun YA. Inhibition of the neutral magnesium-dependent sphingomyelinase by glutathione. *J Biol Chem* 1997; **272**: 16281–16287.
40 Matsushima S, Kinugawa S, Yokota T, Inoue N, Ohta Y, Hamaguchi S, Tsutsui H. Increased myocardial NAD(P)H oxidase-derived superoxide causes the exacerbation of postinfarct heart failure in type 2 diabetes. *Am J Physiol Heart Circ Physiol* 2009; **297**: H409–H416.
41 Yokota T, Kinugawa S, Hirabayashi K, Matsushima S, Inoue N, Ohta Y, Hamaguchi S, Sobirin MA, Ono T, Suga T, Kuroda S, Tanaka S, Terasaki F, Okita K, Tsutsui H. Oxidative stress in skeletal muscle impairs mitochondrial respiration and limits exercise capacity in type 2 diabetic mice. *Am J Physiol Heart Circ Physiol* 2009; **297**: H1069–H1077.
42 Martinez-Revelles S, Caracuel L, Marquez-Martin A, Dantas A, Oliver E, D'Ocon P, Vila E. Increased endothelin-1 vasoconstriction in mesenteric resistance arteries after superior mesenteric ischaemia-reperfusion. *Br J Pharmacol* 2012; **165**: 937–950.
43 Li S, Fang Q, Zhou A, Wu L, Shi A, Cao L, Zhu H, Liu Y, Mao C, Xu Z. Intake of high sucrose during pregnancy altered large-conductance $Ca^{2+}$-activated $K^+$ channels and vessel tone in offspring's mesenteric arteries. *Hypertens Res* 2013; **36**: 158–165.
44 Zhao Y, Flavahan S, Leung SW, Xu A, Vanhoutte PM, Flavahan NA. Elevated pressure causes endothelial dysfunction in mouse carotid arteries by increasing local angiotensin signaling. *Am J Physiol Heart Circ Physiol* 2015; **308**: H358–H363.
45 Wang R, Bi J, Ampah KK, Zhang C, Li Z, Jiao Y, Wang X, Ba X, Zeng X. Lipid raft regulates the initial spreading of melanoma A375 cells by modulating beta1 integrin clustering. *Int J Biochem Cell Biol* 2013; **45**: 1679–1689.
46 Murali S, Zhang M, Nurse CA. Angiotensin II mobilizes intracellular calcium and activates pannexin-1 channels in rat carotid body type II cells via AT1 receptors. *J Physiol* 2014; **592**: 4747–4762.
47 Brilla CG, Scheer C, Rupp H. Angiotensin II and intracellular calcium of adult cardiac fibroblasts. *J Mol Cell Cardiol* 1998; **30**: 1237–1246.
48 De Bock M, Wang N, Decrock E, Bol M, Gadicherla AK, Culot M, Cecchelli R, Bultynck G, Leybaert L. Endothelial calcium dynamics, connexin channels and blood-brain barrier function. *Prog Neurobiol* 2013; **108**: 1–20.
49 Li L, Pang XB, Chen BN, Gao L, Wang L, Wang SB, Wang SB, Liu DP, Du GH. Pinocembrin inhibits angiotensin II-induced vasoconstriction via suppression of the increase of [$Ca^{2+}$]i and ERK1/2 activation through blocking AT(1)R in the rat aorta. *Biochem Biophys Res Commun* 2013; **435**: 69–75.
50 Tapper H, Furuya W, Grinstein S. Localized exocytosis of primary (lysosomal) granules during phagocytosis: role of Ca2+-dependent tyrosine phosphorylation and microtubules. *J Immunol* 2002; **168**: 5287–5296.
51 Cremesti AE, Goni FM, Kolesnick R. Role of sphingomyelinase and ceramide in modulating rafts: do biophysical properties determine biologic outcome? *FEBS Lett* 2002; **531**: 47–53.

52 Touyz RM. Lipid rafts take center stage in endothelial cell redox signaling by death receptors. *Hypertension* 2006; **47**: 16–18.
53 Jin S, Yi F, Zhang F, Poklis JL, Li PL. Lysosomal targeting and trafficking of acid sphingomyelinase to lipid raft platforms in coronary endothelial cells. *Arterioscler Thromb Vasc Biol* 2008; **28**: 2056–2062.
54 Gulbins E, Li PL. Physiological and pathophysiological aspects of ceramide. *Am J Physiol Regul Integr Comp Physiol* 2006; **290**: R11–R26.
55 Tam C, Idone V, Devlin C, Fernandes MC, Flannery A, He X, Schuchman E, Tabas I, Andrews NW. Exocytosis of acid sphingomyelinase by wounded cells promotes endocytosis and plasma membrane repair. *J Cell Biol* 2010; **189**: 1027–1038.
56 Amaddii M, Meister M, Banning A, Tomasovic A, Mooz J, Rajalingam K, Tikkanen R. Flotillin-1/reggie-2 protein plays dual role in activation of receptor-tyrosine kinase/mitogen-activated protein kinase signaling. *J Biol Chem* 2012; **287**: 7265–7278.
57 Wyse BD, Prior IA, Qian H, Morrow IC, Nixon S, Muncke C, Kurzchalia TV, Thomas WG, Parton RG, Hancock JF. Caveolin interacts with the angiotensin II type 1 receptor during exocytic transport but not at the plasma membrane. *J Biol Chem* 2003; **278**: 23738–23746.
58 Liu G, Hitomi H, Rahman A, Nakano D, Mori H, Masaki T, Ma H, Iwamoto T, Kobori H, Nishiyama A. High sodium augments angiotensin II-induced vascular smooth muscle cell proliferation through the ERK 1/2-dependent pathway. *Hypertens Res* 2014; **37**: 13–18.
59 Jaiswal JK, Andrews NW, Simon SM. Membrane proximal lysosomes are the major vesicles responsible for calcium-dependent exocytosis in nonsecretory cells. *J Cell Biol* 2002; **159**: 625–635.
60 Moncada S, Higgs EA. Molecular mechanisms and therapeutic strategies related to nitric oxide. *Faseb J* 1995; **9**: 1319–1330.
61 Fukao M, Hattori Y, Kanno M, Sakuma I, Kitabatake A. Sources of $Ca2^+$ in relation to generation of acetylcholine-induced endothelium-dependent hyperpolarization in rat mesenteric artery. *Br J Pharmacol* 1997; **120**: 1328–1334.
62 Lambert TL, Kent RS, Whorton AR. Bradykinin stimulation of inositol polyphosphate production in porcine aortic endothelial cells. *J Biol Chem* 1986; **261**: 15288–15293.
63 Gomolak JR, Didion SP. Angiotensin II-induced endothelial dysfunction is temporally linked with increases in interleukin-6 and vascular macrophage accumulation. *Front Physiol* 2014; **5**: 396.
64 Seto SW, Krishna SM, Yu H, Liu D, Khosla S, Golledge J. Impaired acetylcholine-induced endothelium-dependent aortic relaxation by caveolin-1 in angiotensin II-infused apolipoprotein-E (ApoE-/-) knockout mice. *PLoS ONE* 2013; **8**: e58481.